International Journal of Industrial Electronics, Control and Optimization © 2020 IECO
Vol. 3, No. 3, pp. 313-326, July (2020)

Security-Constrained Unit Commitment in the Presence of Demand Response Programs and Electric Vehicles

Mohsen Ramezanzadeh[1,†], Meysam Jafari-Nokandi[2], Taghi Barforoushi[3], Javad Saebi[4]
[1, 2, 3] Research Department of HV Stations, Department of Electrical and Computer Engineering, Babol Noshirvani University of Technology, Babol, Iran
[4] Department of Electrical Engineering, University of Bojnord , Bojnord, Iran.

ABSTRACT

In recent years, concerns about environmental pollutions have risen and in this respect, the power system and transportation section have been introduced as the main sources of their emission. Therefore, renewable energy sources (RESs), predominantly wind generation, can be effective for reducing emissions caused by the power system, and electric vehicles (EVs) can be very useful for decreasing emissions in the transportation section. However, RESs are intermittent and uncertain, and on the other hand, high penetration of EVs into the system can be challenging for power system operation. Consequently, the stochastic behavior of RESs and charging demand of EVs should be considered in the daily operation scheduling of generating units that is known as the unit commitment (UC) problem. In this regard, this paper presents a two-stage stochastic programming model for the security-constrained unit commitment (SCUC) taking into account the effect of EVs penetration and wind power integration into the power system. The effect of EV travels on the demand of busses is modeled in the proposed framework. Moreover, the impact of demand response (DR) programs on the operation cost of the system is considered. The results of simulations in a six-bus test system illustrate that high EVs penetration reduces power system security and increases the system operation cost, but DR programs can compensate for these negative effects. Moreover, the increase in cost in a controlled charging mode can be insignificant.

Article Info

Keywords:
Demand Response Program, Electric Vehicle
Security-Constrained Unit Commitment
Stochastic Programming, Uncertainty.

Article History:
Received 20**-**-**-**
Accepted 20**-**-**-**

NOMENCLATURE

Indices:

t, q,d	Indices of time periods (hour)
r	Index of DR providers (DRPs)
k	Index of DRP bidding segments
s	Index of scenarios
j	Index of shiftable loads
e	Index of EVs' trip group
w	Index of wind farms
i	Index of thermal units
n,m	Index of system busses
L	Index of system lines

Parameters:

cc_{rt}^{k}	Scheduling cost of point *k* of the offer package of DRP *r* at time *t* ($/MW)
q_{r}^{k}	*k*th discrete DR reserve (DRR) value of the bid of DRP *r* (MW)
ec_{rts}^{k}	Deployment cost of point *k* of the scheduled offer by DRP *r* at time *t* ($/MWh)
NQ_r	Number of DRP bidding segments
$IP^{t,d}$	Cost of load shifting from period t to d ($/MW)
TPC	The total generation of the power system (KW)

†Corresponding Author: m.jafari@nit.ac.ir
Tel: +98-1135501430, Fax: +98-113234201, Noshirvani University of Technology
Department of Electrical and Computer Engineering, Babol Noshirvani University of Technology, Babol, Iran

APC	The average annual electricity production per capita (kW/cap)
VCF	The vehicle-per-capita factor (vehicles/cap)
CP	The covered population of the power system
PPT_{et}	The percentage of each group to total trips per hour over a 24-h period
TEV	Total electric vehicle
ET_e	Number of EVs in each trip group *e*
EVT_{et}	Number of EVs in group *e* at time *t*
$P_{consume}$	Consumption power of each EV (kW/km)
TL_e	Trip distance of group *e* (km)
EVA_{et}	Battery capacity of the parked EVs in group *e* connected to the grid and available for charging in period *t*
CE_{et}	Consumed energy by EVs in group *e* in period *t*
η_{ch}	Efficiency of battery charging
η_{disch}	Efficiency of battery discharging
BF_e	Battery capacity of EVs in group *e* (MWh)
MT_{et}	Maximum energy that can be transferred to EVs in group *e* in time *t*.
EU_{et}	The charging rate of EVs in base case
SEU_{ets}	The charging rate of EVs in scenarios
CL	Restriction on the power of line that can be transferred to one EV.
σ_{wt}	Standard deviation of wind power forecasting error at time *t*
σ_d	Standard deviation of load forecasting error
T	Time horizon of the scheduling
N_g	Number of thermal units
NDR	Number of demand response providers
Nsl	Number of participants in the shiftable load program
N_w	Number of wind farms
Ns	Number of scenarios
Nb	Number of busses
$C_{g,i}$	Cost of generating energy by unit *i* ($/MWh)
$C_{RR,i}$	Regulation reserve cost of unit *i* ($/MWh)
$C_{SR,i}$	Spinning reserve cost of unit *i* ($/MWh)
$C_{curt,wt}$	Cost of curtailed wind power of unit *w* at time *t* and scenario *s* ($/MWh)
ρ_s	Probability of scenario *s* of wind and load uncertainty
$VOLL_n$	Value of lost load ($/MWh)
Pd_{nt0}	Power demand at bus *n* at time *t* (MW)
Pd_{nts}	Power demand at bus *n* at time *t* and scenario *s* (MW)
$P_{\max,i}$	Maximum generation of unit *i* (MW)
$P_{\min,i}$	Minimum generation of unit *i* (MW)
$RR_{\max,i}$	Maximum regulation reserve of unit *i* (MW)
$SR_{\max,i}$	Maximum Spinning reserve of unit *i* (MW)
$DRR_{\max,r}$	Maximum load that can be reduced by DRP *r* (MW)
$P_{\varphi,wt0}$	Forecasted wind power of unit *w* at time *t* (MW/h)
γ	Maximum power that can be shifted by responsible load at shiftable load program (MW)
UR_i	Ramp up limit (MW)
DR_i	Ramp down limit (MW)
DT_i	Minimum down time for unit *i* (h)
UT_i	Minimum up time for unit *i* (h)
B_L	Susceptance of line *L* (p.u)
$f_{\max,L}$	Maximum power that can be transferred from line L (MW)
$\theta_{\max}$	Maximum voltage angel of busses (rad)
$P_{\varphi,wts}$	The forecasted power of wind farm *w* at time *t* and scenario *s* (MW)
$LC_{\max,n}$	Maximum involuntary load shedding at bus *n* (MW)

Variables:

DRR_{rt}	Scheduled demand response reserve by DRP *r* at time *t* (MW)
DRR_{rts}	Deployed demand response reserve by DRP *r* at time *t* and scenario *s* (MW)
$CDRR_{rt}$	Cost of scheduling DRR by DRP *r* at time *t* ($/MW)
$CEDRR_{rts}$	Cost of deployed DRR by DRP *r* at time *t* and scenario *s* ($/MW)
u_{rt}^k	Binary variable associated with scheduling point of DRP *r* at time *t*, which is 1 if the point is scheduled and 0 otherwise.
u_{rts}^k	Binary variable associated with deployment point of DRP *r* at time *t* and scenario s, which is 1 if the point is scheduled and 0 otherwise.
λ_r^k	The quantity of bidding segments of DR providers
$SL_{j0}^{t,d}$	Scheduled shiftable load *j* from hour *t* to *d* (MW)
$SL_{js}^{t,d}$	Deployed shiftable load *j* from *t* to *d* at scenario *s* (MW)
$CSL_{j0}^{t,d}$	Cost of scheduled shiftable load *j* from *t* to *d* ($/MW)
$CSL_{js}^{t,d}$	Cost of deployed shiftable load *j* from *t* to *d* at scenario *s* ($/MW)
f_1	The operation cost of the system in the base case
f_2	The expected costs corresponding to scenarios
P_{it0}	Scheduled generation power of unit *i* at time *t*

	(MW)
$RR_{u,it}$	Scheduled regulation-up reserve of unit *i* at time *t* (MW)
$RR_{dn,it}$	Scheduled regulation-down reserve of unit *i* at time *t* (MW)
$SR_{u,it}$	Scheduled spinning-up reserve of unit *i* at time *t* (MW)
$SR_{dn,it}$	Scheduled spinning-down reserve of unit *i* at time *t* (MW)
SU_{it}	Startup cost of unit *i* at time *t* ($)
SD_{it}	Shutdown cost of unit *i* at time *t* ($)
$P_{curt,wt0}$	Curtailed wind generation of unit *w* at time *t* (MW)
$P_{curt,wts}$	Curtailed wind generation of unit *w* at time *t* and scenario *s* (MW)
P_{its}	Power generation of unit *i* at time *t* and scenario *s* (MW)
RR_{its}	Deployed regulation reserve of unit *i* at time *t* in scenario *s* (MW)
SR_{its}	Deployed spinning reserve of unit *i* at time *t* in scenario *s* (MW)
LC_{nts}	Involuntary load shedding at bus *n* and time *t* in scenario *s* (MW)
$f_{L,nm,t0}$	Power flow of line *L* from bus *n* to *m* at time *t* (MW)
$f_{L,nm,ts}$	Power flow of line *L* from bus *n* to *m* at time *t* in scenario *s* (MW)
I_{it}	Commitment state of unit *i* at time *t*
P_{wt0}	Scheduled generation of wind farm *w* at time *t* (MW)
P_{wts}	Generation of unit *w* at time *t* and scenario *s* (MW)
y_{it}	Startup indicator, which is 1 if unit *i* is started up at time *t* and 0, otherwise.
z_{it}	Shut down indicator, which is 1 if unit *i* is shut down at time *t*.
θ_{nt0}	Voltage angle of bus *n* at time *t* (rad)
θ_{nts}	Voltage angle of bus *n* at time *t* and scenario *s* (rad)
SOC_{et}	The state of charge of each group of EVs
$SSOC_{ets}$	The state of charge of each group of EVs in each scenario

I. INTRODUCTION

Security-constrained unit commitment (SCUC) is the problem of determining the on/off state of thermal units taking into account the technical limitations of generating units and transmission lines. Traditionally, the SCUC problem is solved to minimize total operation cost for supplying system demand. The operation cost includes the production cost of generating units and their start-up and shut-down cost.

Nowadays, environmental concerns associated with the use of fossil fuels in the power systems have led to a worldwide shift of focus to the use of RESs [1]. Wind energy in comparison to other renewable energies plays an important role since it is relatively cheap and efficient to reduce emissions. However, wind power is intermittent and uncertain which force the power system to operate with more spinning reserve to compensate for wind power volatility.

Another cause of environmental pollutions is the transportation section where vehicles have internal combustion engines. Therefore, many governments and automobile manufacturers focus on the use of electrical engines instead of combustion ones [2]. But, the growth of electric vehicles (EVs) number puts stress on the power system to provide their charging demand. It may result in the commitment of more expensive generating units which increase the operation cost of the power system. On the other hand, consumer participation in demand response (DR) programs greatly helps the power system for optimal using of energy resources [3]. Market experiences have shown that the use of DR programs has many benefits for consumers, the electricity market, and the grid. The consumers' benefits include economic benefits and continuity in electricity supply. From the market viewpoint, DR can prevent price volatility and for the grid, the benefit is saving the investment costs, postponing the construction of new power plants, and shaving the peak load [4]. However, the SCUC problem incorporating RESs, EVs and DR programs will be a complex and large-scale problem [5].

Recently, more attention has been paid to model the presence of RESs and EVs in the SCUC problem to reduce environmental emissions and dependency on fossil fuels [6-8]. In [9], a two-stage robust SCUC model is presented for managing wind power uncertainty in the hourly power system scheduling wherein the operation cost is minimized. In [10], a novel model is proposed for optimizing the spinning reserve requirement considering EVs' contribution to the power system for providing the operating reserve. In [11], a pool-based DR exchange model is proposed in which, an economic DR is traded among DR participants as a solution for managing the variability of RES. Load curtailment bids are provided by individual DR exchange participants and these bids are cleared to maximize the social welfare problem, simultaneously. Reference [12] studies the impacts of EV charging patterns on power system operation and scheduling. A stochastic UC model is presented that considers the coordination of thermal generating units and EV charging demand, as well as the large-scale penetration of wind power. The proposed model also addresses the ancillary services provided by vehicle-to-grid (V2G) technology. In [13], hourly coordination of EVs charging and volatile wind power generation are studied via SCUC wherein the expected operation cost is minimized. In [14], modeling the traffic flow of PEVs is studied in which, Different travel types and purposes are considered. Two types of charging infrastructure (i.e., parking lots and individual charging stations) are taking into account. The study is performed on a distribution network while RES, load uncertainty, and DR are not considered. A mixed-integer linear programming (MILP) model is presented in [15] with the focus on the effect of EVs on the generation side. However, traveling patterns of EVs, RES, load uncertainty and DR were not considered in [15]. In [16], the effect of wind power and load

forecast errors are considered in the stochastic SCUC problem using a two-stage stochastic programming model. DR is utilized as a tool for mitigating transmission violations in the presence of uncertainties. However, EVs are not considered. In [17], the influence of DR program on the system economy and security indices in uncertain conditions of wind power and load is investigated without considering the presence of EVs.

In [18], robust and stochastic optimizations are introduced as efficient tools for mitigating wind power uncertainties. A single-level MILP robust UC is presented and compared with the common robust formulation. It shows that the proposed method is faster than the traditional one. In [19], a new form of UC is presented for investigating renewable generation uncertainties considering PEVs for managing wind power uncertainty. Reference [20] presents a heuristic technique based on a priority list for solving the SCUC problem. Day-ahead scheduling is performed under solar, wind, and arrival/ departure time of PHVs uncertainties. Day-ahead scheduling of power system under wind uncertainty is formulated in [21] that determines the optimal number of EVs which should present in parking at each hour. The results demonstrate that the co-operation of V2G and wind farms reduce daily operation cost and increases network reliability. Reference [22] determines the optimal management of charging and discharging of EVs in parking stations for reducing daily operation cost in the SCUC problem without considering uncertainties. Furthermore, the results show that if the value of the EVs penetration level be higher than a specified level, the operation cost will remain constant due to the price of the power generated by EVs and the power line flow limits. Reference [23] presents a SCUC problem that includes thermal and nuclear power plants, wind farm, and energy storage system. The storage system is applied for mitigating wind power uncertainty. The results show the performance of the model in reducing operation cost and peak shaving. However, none of the abovementioned researches consider the DR programs in the SCUC problem in a power system with high EV penetration.

In [24], a SCUC problem is proposed in the presence of the high penetration of wind energy. The presented model applies DR program and energy storage for reducing the effect of wind uncertainties. A stochastic SCUC is presented in [25] which includes wind power, hydrogen energy storage, and price-based DR. the results indicate that the simultaneous participation of DR program, energy storages, and wind power reduce wind spillage and daily operation cost. In this study, EVs are not taking into account. [26] proposes the stochastic UC problem based on a multi-scenario tree method. The load and wind uncertainties are considered for determining the reserve requirements but DR program and EVs are not considered.

According to the literature review, there is not a comprehensive study that addresses the challenge of the simultaneous presence of EVs and DR programs in the SCUC problem. The dramatic increase in the number of EVs in the power system has a major impact on the SCUC problem. The reason is due to the considering the following factors in the optimization problem of the SCUC: 1) a high number of decision variables that model the EVs 2) high amount of movable loads for representing the EVs. To cope with the mentioned issues, in this paper a stochastic SCUC is developed, in which EVs are modeled as mobile loads without adding much decision variables into the problem (the high number of decision variables for modeling the EVs in [13] makes the solving of the SCUC problem a challenging task). In the proposed framework, the uncertainties of wind power and load are included. A developed model for integrating a large number of EVs into power systems has been employed based on the method presented in [15]. The developed stochastic model is more suitable for utilizing in a stochastic SCUC than what introduced in [15]. Moreover, considering the EVs traveling patterns among the system busses in the developed model makes it possible to examine the effect of the EVs load on the occurrence of transmission lines congestion and consequently on the energy and reserve scheduling, which are not addressed in [15]. In the presented model, the charging time and charging demand of EVs are divided into different groups based on the length and type of their trips. Moreover, the origin and destination of the trips are taking into account for modeling the effect of trips on the load of system busses. The contributions of this paper are as follows:

- Developing a stochastic SCUC model in order to study the effect of large-scale integration of EVs into a power system.
- Extending the EVs model into the stochastic model by considering the traveling pattern and the impact of EVs flows on the hourly load of system busses.
- Studying the effect of DR on the penetration level of EVs and also on the power system operating cost.

Section II deals with the mathematical formulation of the problem. Simulation results of the proposed model and sensitivity analyses are presented in section III, and section IV concludes the results.

II. MATHEMATICAL MODEL

The proposed model for the SCUC problem takes into account several components including DR programs, the uncertainties of wind power and load, and the effect of EVs of system demand. In this section, mathematical modeling for these components is presented. Then, the SCUC model is expressed as a stochastic programming problem.

A. Modeling of DR programs

In this paper, it is assumed that consumers can participate in two different DR programs. In the former, participants are reserve providers, and they may reduce a part of their demand in case of necessity. In the latter, DR providers emerge as shiftable loads (SL) and can transfer a percentage of their demand from the peak periods (with high prices) to

the off-peak periods (with low prices).

1) Reserve providers

In this DR program, reserve providers propose their offer packages containing capacity and price discretely to the Independent System Operator (ISO) [16]. As shown in Fig. 1, each block of the offer is fully accepted or rejected and is fully utilized at the required time. The term “X" denotes the acceptance of the offer for each part in the scheduling stage, and "+" denotes the deployment of the discrete DR offer in scenarios.

$$DRR_{rt} = \sum_{k=1}^{NQ_r} \lambda_r^k u_{rt}^k \qquad \forall r, \forall t \qquad (1)$$

$$CDRR_{rt} = \sum_{k=1}^{NQ_r} cc_{rt}^k \lambda_r^k u_{rt}^k \qquad \forall r, \forall t \qquad (2)$$

$$DRR_{rts} = \sum_{k=1}^{NQ_r} \lambda_r^k u_{rts}^k \qquad \forall r, \forall t, \forall s \qquad (3)$$

$$CEDRR_{rts} = \sum_{k=1}^{NQ_r} ec_{rts}^k \lambda_r^k u_{rts}^k \qquad \forall r, \forall t, \forall s \qquad (4)$$

$$\lambda_r^k = q_r^k - q_r^{k-1} \qquad \forall r, \forall k \qquad (5)$$

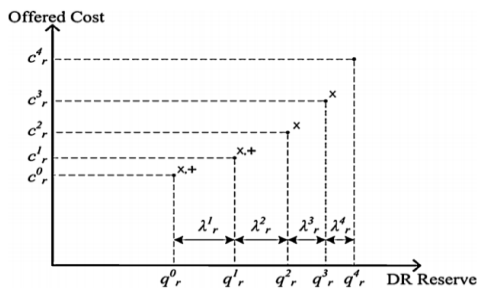


Fig. 1. Discrete DR bid scheduling and deployment [16].

2) Shiftable loads

The presented model of SLs is considered to relieve the stresses on the grid in the peak load hours. The ISO can procure this service based on load forecast by providing incentives for consumers to shift a part of their demand from peak periods to the off-peak periods. It is assumed that a percentage of the available load in each bus can be called for the load shifting. Equs. (6) and (7) show the procurement cost of this DR program for shifting load from hour *t* to hour *d* in the base case and scenarios [17]:

$$CSL_{j0}^{t,d} = SL_{j0}^{t,d} IP^{t,d} \qquad \forall j, \forall t, d \qquad t \neq d \qquad (6)$$

$$CSL_{js}^{t,d} = SL_{js}^{t,d} IP^{t,d} \qquad \forall j, \forall t, d, \forall s \qquad t \neq d \qquad (7)$$

B. Modeling the uncertainties of wind power and load

Forecast errors of wind power and load are considered as normal distributions, which are shown by $N(P_{\varphi,wt0}, \sigma_{wt}^2)$ and $N(P_{dto}, \sigma_d^2)$, respectively. In these forecast models, $P_{\varphi,wt0}$ and P_{dt0} are the forecasted wind power and the forecasted system load at time *t*, respectively; σ_{wt} and σ_d represent the wind and load volatility, respectively. The autocorrelation of the wind and the load forecast error models are assumed to be zero and the wind and load uncertainties are assumed independent [26].

C. Modeling the effect of EVs on system load

The dramatic increase in the number of EVs could have a major impact on power system operation. Thus, the effect of EVs' charging demand on the load of busses should be taken into account in power system scheduling. Here, it is assumed that a distribution company (DISCO) submits the information of EV groups to the ISO for considering in the day-ahead market. The information of EVs includes starting locations and destination of the trips, departure and arrival times at designated locations, and the charging/discharging capacity of EVs which can be coupled with power system operations [13].

Usually, EVs are considered in the UC model as mobile electrical storage units, which are charged and discharged over the scheduling horizon. However, modeling the individual performance of every EV requires that each EV be denoted with a decision variable [13]. On the one hand, this approach dramatically increases the size of the optimization problem in large-scale systems with a high number of EVs. On the other hand, as the focus of the presented study is on the effect of EVs penetration on the generation side and the additional power generation, the individual performance of every EV becomes less importance here [27]. In this state, what is really significant is the amount of electric energy that should be transferred to all EVs in the system at every hour of the day so that their batteries will be full in the next morning [15]. Therefore, in the current work, an aggregated model for EVs is used that considers EVs as mobile loads. In the presented model, the charging time and the charging demand of EVs are divided into different groups based on the length and type of their trips. Moreover, the origin and destination of the trips are taking into account for modeling the effect of trips on the load of system busses, which then can be used by the ISO in the market clearing process.

For modeling EVs, first, it is needed to use the specified daily travel profiles which can be obtained by the Institute for Transport and Communications of every country. In this model, in addition to the introduction of different types of travel within the context of the diverse groups (which in the current study, they are shown by e index), the percentage of them to total trips (PPT_{et}) should be obvious as well. Secondly, regarding the total generation of the power system (TPC) and the average annual electricity production per capita (APC) and the division of TPC to APC, the covered population (CP) of the power system is determined as expressed by Equ. (8):

$$CP = \frac{TPC}{APC} \qquad (8)$$

Thirdly, by having the vehicle-per-capita factor (VCF) and multiplying it by the population obtained from the Equ. (8), the

total number of EV (TEV) in that system is determined which is calculated by Equ. (9):

$$VCF \times CP = TEV \tag{9}$$

Finally, by multiplying TEV by PPT_{et}, the number of trips started per hour for each group e can be calculated (ET_e). Therefore, in this way, it is possible to determine the number of parked EVs in group e connected to the grid and available for charging in each time slot t. Consequently, the daily energy consumption for each group during the trips and EVs' corresponding battery capacities as input parameters of SCUC problem can be calculated by Equs. (10) and (11), respectively:

$$CE_{et} = EVT_{et}.P_{consume}.TL_e \qquad \forall e, \forall t \tag{10}$$

$$EVA_{et} = ET_e.BF_e - CE_{et} \qquad \forall e, \forall t \tag{11}$$

D. Formulation of the SCUC Problem with EVs and DR

In this section, the mathematical formulation of the proposed model is presented in the form of a two-stage stochastic optimization problem.

Equ. (12) shows the objective function that includes two terms. The first term represents the operation cost of the system in the base case which is formulated as (13). It consists of the production cost of generating units, the startup and shutdown costs, the cost of up and down regulation and spinning reserve, the cost of wind energy curtailment, and the cost of DR services supplied by reserve providers and shiftable loads. Equ. (14) demonstrates the expected costs of deployment of regulation and spinning reserves and DR services, and the expected cost of involuntary load shedding and wind power curtailment regarding the realized scenarios.

$$\min f_1 + f_2 \tag{12}$$

$$f_1 = \sum_{t=1}^{T}\left\{\sum_{i=1}^{N_g}\begin{bmatrix} C_{g,i}P_{it0} + SU_{it} + SD_{it} \\ +C_{RR,i}RR_{u,it} + C_{RR,i}RR_{d,it} \\ +C_{SR,i}SR_{u,it} + C_{SR,i}SR_{d,it}\end{bmatrix}\right. \\ \left. + \sum_{w=1}^{N_w} P_{curt,wto}.C_{curt,wt} \right. \\ \left. + \sum_{r=1}^{NDR} CDRR_{rt} + \sum_{t,d}\sum_{j=1}^{Nsl} CSL_{j0}^{t,d}\right\} \tag{13}$$

$$f_2 = \sum_{t=1}^{T}\sum_{s=1}^{Ns}\left\{\rho_s\sum_{i=1}^{N_g}\left(C_{g,i}P_{its} - C_{g,i}P_{it0}\right) + \sum_{r=1}^{NDR} CEDRR_{rts}\right. \\ \left. + \sum_{t,d}\sum_{j=1}^{N_{sl}} CSL_{js}^{t,d} + \sum_{n=1}^{Nb} VOLL_n LC_{nts} + \sum_{w=1}^{N_w} P_{curt,wts}.C_{curt,wt}\right\} \tag{14}$$

The above objective function should be optimized subjected to two categories of constraints:

1) *First stage constraints*

The first stage constraints are related to the here-and-now decisions, in which, decisions on generating units on/off states and the scheduled energy and reserve in the market are made. Equation (15) shows the balance between power generation and consumption in each bus:

$$\sum_{i\in n} P_{it0} + P_{wt0} - \sum_{\substack{m=1 \\ L\in n}} f_{L,nm,t0} - \sum_{e\in n} EU_{e,t} \\ = Pd_{nt0} - \sum_{j\in n} SL_{j0}^{t,d} + \sum_{j\in n} SL_{j0}^{d,t} \qquad \forall t \tag{15}$$

where the wind power production is considered zero for those busses that are without wind farm.

Unit generation, generation-side reserves, and wind power curtailment constraints are expressed by Equs. (16)-(24), respectively. Equs. (16) and (17) imply the allocated production plus the up or down reserves of each generating unit should be between the minimum and maximum production capacity of each unit. Equs. (18)-(20) limit the regulation reserves and spinning reserves to the ramp rate limitation of each generating unit. Equ. (22) limits the scheduled DR reserves to the maximum offered by DR providers. According to (23), the maximum scheduled wind power production is equal to the predicted wind power. In (24) the wind curtailment in the base case is calculated. Maximum load that can be transferred for shiftable loads is expressed by (25). Equ. (26) shows that the same amount of the shifted load from an hour will be added to the load demand at the target hour:

$$P_{it0} + RR_{u,it} + SR_{u,it} \le P_{\max,i} I_{it} \qquad \forall i, \forall t \tag{16}$$

$$P_{it0} - RR_{dn,it} - SR_{dn,it} \ge P_{\min,i} I_{it} \qquad \forall i, \forall t \tag{17}$$

$$0 \le RR_{u,it} \le RR_{\max,i} \qquad \forall i, \forall t \tag{18}$$

$$0 \le RR_{dn,it} \le RR_{\max,i} \qquad \forall i, \forall t \tag{19}$$

$$0 \le SR_{u,it} \le SR_{\max,i} \qquad \forall i, \forall t \tag{20}$$

$$0 \le SR_{dn,it} \le SR_{\max,i} \qquad \forall i, \forall t \tag{21}$$

$$0 \le DRR_{rt} \le DRR_{\max,r} \qquad \forall r, \forall t \tag{22}$$

$$0 \le P_{wt0} \le P_{\varphi,wt0} \qquad \forall w, \forall t \tag{23}$$

$$P_{curt,wt0} = P_{\varphi,wt0} - P_{wt0} \qquad \forall w, \forall t \tag{24}$$

$$0 \le SL_{j0}^{t,d} \le \gamma Pd_{rt0} \qquad \forall j, \forall r, \forall t, d \qquad t \ne d \tag{25}$$

$$SL_{j0}^{t,d} = -SL_{j0}^{d,t} \qquad \forall j, \forall t, d \qquad t \ne d \tag{26}$$

According to (27) and (28), if a thermal unit is committed for two consecutive hours, maximum increase or decrease of its hourly production is limited to UR_i and DR_i, respectively. However, if the unit is starting up, its production at the next hour will reach to P_{min}, and if the unit is shutting down, its production should reach P_{min} at the previous hour [16]. Equs. (29)-(32) determine the value of binary variables corresponding to start up and shut down of thermal units. In (33) and (34), minimum up/off time limits are indicated [28]:

$$P_{it0} - P_{i(t-1)0} \le (1 - y_{it})UR_i + y_{it}P_{\min,i} \qquad \forall i, \forall t \tag{27}$$

$$P_{i(t-1)0} - P_{it0} \le (1 - z_{it})DR_i + z_{it}P_{\min,i} \qquad \forall i, \forall t \qquad (28)$$

$$y_{it} - z_{it} \le I_{it} - I_{i(t-1)} \qquad \forall i, \forall t \qquad (29)$$

$$y_{it} + z_{it} \le 1 \qquad \forall i, \forall t \qquad (30)$$

$$0 \le y_{it} \le 1 \qquad \forall i, \forall t \qquad (31)$$

$$0 \le z_{it} \le 1 \qquad \forall i, \forall t \qquad (32)$$

$$\sum_{q=t-UT_i+1}^{t} y_{it} \le I_{it} \qquad \forall i, \forall t \in \{UT_i, ..., T\} \qquad (33)$$

$$\sum_{q=t-DT_i+1}^{t} z_{it} \le 1 - I_{it} \qquad \forall i, \forall t \in \{DT_i, ..., T\} \qquad (34)$$

Power flows of the transmission lines are calculated by DC load flow as shown by (35). Equs. (36) and (37) limit the power flow of lines and voltage angle of busses to their minimum and maximum value, respectively:

$$f_{L,nm,t0} = B_L(\theta_{nt0} - \theta_{mt0}) \qquad \forall L, \forall m, \forall n, \forall t \quad m \ne n \qquad (35)$$

$$-f_{\max,L} \le f_{L,nm,t0} \le f_{\max,L} \qquad \forall L, \forall m, \forall n, \forall t \quad m \ne n \qquad (36)$$

$$-\theta_{\max} \le \theta_{nt0} \le \theta_{\max} \qquad \forall n, \forall t \qquad (37)$$

According to (38), all EVs must be fully charged at the start time of their trip. Regarding the charging or discharging mode, the state of charge (SOC) of each group of EVs is expressed by (39). According to (40), the SOC of EV groups should be less than their maximum capacity. Equs (41) describes that the charging rate of EVs is less than a certain amount corresponding to technical constraints. Equ. (42) expresses that the maximum of transferred energy to the batteries is equal to the product of the number of the EVs available for charging and the capacity of the charging lines.

$$SOC_{es} = BF_e \qquad \forall e \in E,\ s = StartHour \qquad (38)$$

$$SOC_{et} = SOC_{e(t-1)} + \eta_{ch}.EU_{et} - \frac{1}{\eta_{disch}}.CE_{et} \qquad \forall e \in E, \forall t \in T \qquad (39)$$

$$0 \le SOC_{e(t-1)} + EU_{et} \le BF_e \qquad \forall e, \forall t \qquad (40)$$

$$EU_{et} \le MT_{et} \qquad \forall e, \forall t \qquad (41)$$

$$MT_{et} = EVA_{et}.CL \qquad \forall e, \forall t \qquad (42)$$

2) *Second stage constraints*

The second stage constraints are related to the real-time operation of the system, in which the wind power and load scenarios are realized. These constraints are briefly described by Equs. (43)-(59):

Power balance at each bus for each time and scenario:

$$\sum_{i \in n} P_{its} + P_{wts} + \sum_{r \in n} DRR_{rts} - \sum_{\substack{m=1 \\ L \in n}} f_{L,nm,ts} - \sum_{e \in n} SEU_{ets} = Pd_{nts} - \sum_{j \in n} SL_{j0}^{t,d} + \sum_{j \in n} SL_{j0}^{d,t} - LC_{nts} \qquad \forall t, \forall s \qquad (43)$$

Output power of generating units and the deployed reserve of DR for each time and scenario:

$$P_{its} = P_{it0} + RR_{its} + SR_{its} \qquad \forall i, \forall t, \forall s \qquad (44)$$

$$-RR_{dn,it} \le RR_{its} \le RR_{u,it} \qquad \forall i, \forall t, \forall s \qquad (45)$$

$$-SR_{dn,it} \le SR_{its} \le SR_{u,it} \qquad \forall i, \forall t, \forall s \qquad (46)$$

$$0 \le DRR_{rts} \le DRR_{rt} \qquad \forall r, \forall t, \forall s \qquad (47)$$

Maximum involuntary load shedding and utilization of the wind power and the wind power curtailment for each time and scenario:

$$0 \le LC_{nts} \le LC_{\max,n} \qquad \forall n, \forall t \qquad (48)$$

$$0 \le P_{wts} \le P_{\varphi,wts} \qquad \forall w, \forall t, \forall s \qquad (49)$$

$$P_{curt,wts} = P_{\varphi,wts} - P_{wts} \qquad \forall w, \forall t, \forall s \qquad (50)$$

Ramp up/down limits of generating units for each time and scenario:

$$P_{its} - P_{i(t-1)s} \le (1 - y_{it})UR_i + y_{it}P_{\min,i} \qquad \forall i, \forall t, \forall s \qquad (51)$$

$$P_{i(t-1)s} - P_{its} \le (1 - z_{it})DR_i + z_{it}P_{\min,i} \qquad \forall i, \forall t, \forall s \qquad (52)$$

SOC of EV groups in each time and scenario:

$$SSOC_{ets} = SSOC_{e(t-1)s} + \eta_{ch}.SEU_{ets} - \frac{1}{\eta_{disch}}.CE_{et} \qquad \forall e \in E, \forall t, \forall s \qquad (53)$$

$$0 \le SSOC_{ets} \le BF_e \qquad \forall e, \forall t, \forall s \qquad (54)$$

$$SEU_{ets} \le MT_{et} \qquad \forall e \in E, \forall t, \forall s \qquad (55)$$

$$MT_{et} = EVA_{et}.CL \qquad \forall e, \forall t, \forall s \qquad (56)$$

Power flow of lines for each time and scenario:

$$f_{L,nm,ts} = B_L(\theta_{nts} - \theta_{mts}) \qquad \forall L, \forall m, \forall n, \forall t, \forall s \quad m \ne n \qquad (57)$$

$$-f_{\max,L} \le f_{L,nm,ts} \le f_{\max,L} \qquad \forall L, \forall m, \forall n, \forall t, \forall s \quad m \ne n \qquad (58)$$

$$-\theta_{\max} \le \theta_{nts} \le \theta_{\max} \qquad \forall n, \forall t, \forall s \qquad (59)$$

III. CASE STUDIES

The proposed model, which was formulated as a MILP problem, was implemented in GAMS environment and solved using CPLEX 12.0. The case studies were carried out on a personal computer with a 2.4 GHz CPU and 4 GB of RAM.

A. *Information of test system*

1) *Generators and lines data*

The six-bus test system shown in Fig. 2, is considered in the presence of a 20 MW wind farm at Bus 6. Parameters of transmission lines and generating units are given in Tables I and II, respectively. Moreover, the value of lost load (VOLL) is assumed to be 450 $/MWh at each load bus and the wind curtailment cost is considered 50 $/MWh. Also, SL and demand-side reserve providers are available at each load bus.

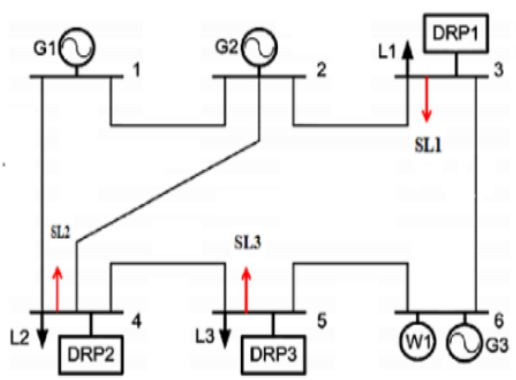


Fig. 2. Single-line diagram of the six-bus system.

TABLE I
PARAMETERS OF LINES

Line No.	Flow Limit MW)	From Bus	To Bus	X (p.u.)
1	200	1	2	0.170
2	150	1	4	0.258
3	150	2	4	0.197
4	100	5	6	0.140
5	135	2	3	0.037
6	120	4	5	0.037
7	100	3	6	0.018

TABLE II
PARAMETERS OF THERMAL UNITS

unit	i_1	i_2	i_3
Location (Bus No.)	1	2	6
Maximum Capacity (MW)	230	100	10
Minimum Capacity (MW)	90	10	0
Maximum Spinning Reserve (MW)	8.35	6.67	5.20
Maximum Regulation Reserve (MW)	8.35	6.67	2.50
Ramp up Limit (MW/h)	50	40	10
Ramp down Limit (MW/h)	50	40	10
Operation Cost ($/MWh)	18.5	49	30
Spinning Reserve Cost ($/MW)	11	10	8
Regulation Reserve Cost ($/MW)	14	13	11
Minimum on Time (h)	4	2	1
Minimum off Time (h)	4	3	1
Start-up Cost ($)	124.69	373.83	0

2) Wind power and load scenarios

The standard deviation of the system load forecast error is assumed 3% of the load forecast at each hour, while the standard deviation of the wind power forecast error increases linearly from 0% to 6.5% of the forecasted power from hour 1 to 24 [16]. Therefore, taking into account the wind unit specifications [29] and using Monte Carlo simulation, 1000 random scenarios were generated corresponding to wind and load forecast errors. The number of scenarios is then reduced to 10 by the fast-backward method [30]. The considered scenarios for wind power and load around their forecasted values are depicted in Fig. 3 and Fig. 4, respectively. Also, the probability of scenarios is given in Table III.

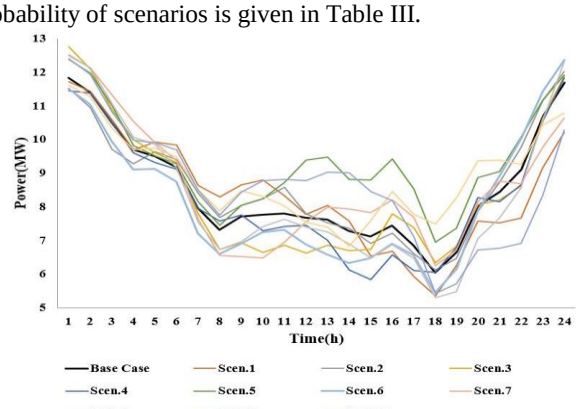


Fig. 3. Wind power forecast scenarios.

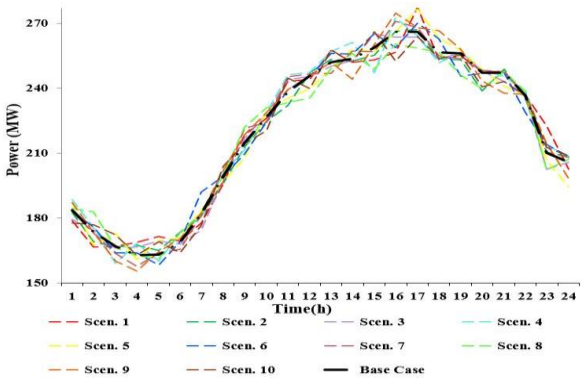


Fig. 4. Load forecast scenarios.

TABLE III
PROBABILITY OF LOAD AND WIND FORECASTING SCENARIOS

scenario	1	2	3	4	5
probability	0.26	0.12	0.08	0.07	0.14
scenario	6	7	8	9	10
probability	0.09	0.02	0.07	0.07	0.08

B. Information of DR programs

1) DR reserve data

In the present study, DRP bids consist of three discrete points for the scheduling stage and scenarios at each time interval that can be seen in Table IV.

TABLE IV
DEMAND RESPONSE RESERVE BIDS

Demand Response Reserve	Bid. 1	Bid. 2	Bid. 3
Maximum Reserve capacity (MW)	1.8	3.6	5.8
Scheduling Cost ($/MW)	10	13	16
Deployment Cost ($/MWh)	10	10	10

2) Shiftable load data

Table V provides information about the shiftable load to participate in the SCUC problem. In this model, according to the load profile of the six-bus test system, ISO determined the hours from 15 to 19 as the peak period and the hours from 3 to 6 as the off-peak period. Also, the maximum load that can be transferred for shiftable loads is equal to 20% of the peak period loads in each load busses.

TABLE V
PARAMETERS OF SHIFTABLE LOADS [17]

Shiftable Load	From Time (t)	To Time (d)	Incentive price ($/MWh)
$SL_j^{15,3}$	15	3	7
$SL_j^{16,5}$	16	5	7
$SL_j^{17,4}$	17	4	7
$SL_j^{18,4}$	18	4	3
$SL_j^{19,6}$	19	6	3

C. EVs' data

Here, the daily Sweden travel pattern for the EVs reported in [15] is utilized. In [15], seven groups of travel (Business, work, study, service, shopping, leisure, and other purposes) are considered. The distribution of the trip-starting times throughout a typical day, which is expressed in the percentage of all trips can be seen in Fig. 5. Moreover, the following assumptions are made:

- All of the trips are for EVs and Because of the small number of trips from 23:00 to 06:00, in the current paper, it is assumed that no trips are started in this period.
- All groups have a two-way trip (leave home in the morning and travel back in the evening) except the last group (other purposes) that has a one-way trip.

Furthermore, as typical data, the average annual electricity production per capita can be roughly approximated by 1 kW/cap [15]; therefore, regarding the 340 MW generation capacity of the six-bus test system used in the simulations, the covered population of the system is estimated at 340000 people (Equ. (8)). If the vehicle-per-capita factor is assumed 0.45 vehicle/cap as a moderate value, the number of vehicles will be about 153000 (Equ. (9)). Thus, knowing the number of vehicles and the driving pattern of group e over the 24-hour time horizon, ET_e can be obtained which as shown in Fig. 6.

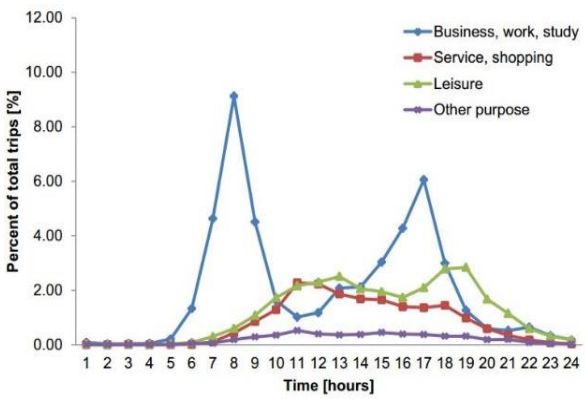


Fig. 5. Starting time of different types of trips over a 24-h period [15].

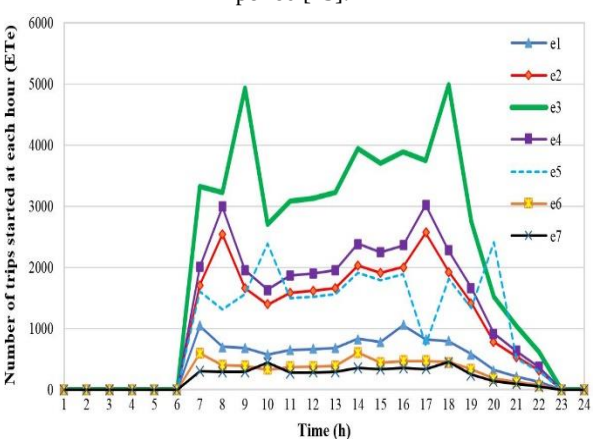


Fig. 6. The number of trips started per hour for each group e

Table VI shows the length of trips in each group. Also, the parameters of EVs and EV groups travel characteristics for six-bus test system can be seen in Tables VII and VIII, respectively.

TABLE VI
TRIP LENGTH OF EV GROUPS (KM) [15]

Groups of EV	e1	e2	e3	e4	e5	e6	e7
Trip length (km)	1.6	3.2	8	16	40	80	160

TABLE VII
PARAMETERS OF THE EVS [31]

EV type	Fully electric vehicle
Battery size	35 kWh
Consumption	0.175 kWh/km
Power line	3 kW
Charge/discharge efficiency	86 %

TABLE VIII
EV GROUPS TRAVEL CHARACTERISTICS

No. Groups	No. EVs	First Trip				Second Trip			
		Arrival		Departure		Arrival		Departure	
		Bus	Time	Bus	time	Bus	Time	Bus	Time
1	9865	6	9	3	8	3	17	6	16
2	23958	1	8	4	7	4	18	1	17
3	46508	6	10	5	9	5	22	6	21
4	28186	5	9	4	8	4	15	5	14
5	22549	2	11	4	10	4	16	2	15
6	5637	4	7	5	6	5	16	4	15
7	4228	3	9	5	7				

D. Case studies

The simulations are carried out for the following cases:

Case 1: Base case (without DR programs and EVs)

Case 2: Presence of EVs without considering their travel pattern

Case 3: Presence of EVs considering their travel pattern

Case 4: Presence of EVs and reserve DR programs

Case 5: With DR programs and controlled charging of EVs

1) Case 1

In this case, generation and reserve are simultaneously scheduled under uncertainties of wind power and load demand. The generation-side reserve is utilized for managing uncertainties, and the involuntary load shedding is applied in the case of reserve insufficiency. The total operation cost, in this case, is 102074.62 $ [16]. Fig. 7 depicts the energy dispatch of generating units. Generators 1, 2, and 3 supply 42.8%, 32.1% and 25.1% of the reserve requirement, respectively.

2) Case 2

In this case, the hourly charging demand of 10,000 EVs is added to the system load. The EVs model utilized in this case is as suggested in [15], i.e. the EVs traveling among the power

system busses and the power flow constraints are not considered. The EVs' load is added to the total system load which affects the balance between the total power generation and consumption in each hour. Therefore, to supply the increased load, Generator 1 produces more energy in comparison to Case 1 and hence its scheduled reserve is decreased. This decrement in the reserve of Generator 1 is compensated by Generator 2. Consequently, the allocation of reserve among the generators 1, 2 and 3 is 39.94%, 34.97%, and 25.09%, respectively, which shows a small decrease in the reserve of Generator 1 and an increase in the scheduled reserve from Generator 2 (in comparison to Case 1). In this case, the operation cost is 104394.32 $ that, in comparison to Case 1, is increased by 2.27% due to the charging demand of EVs and more procurement of reserves.

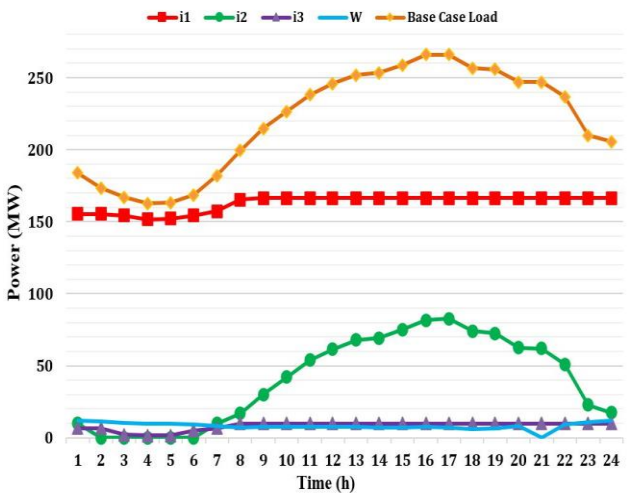


Fig. 7. Generation dispatch in Case 1.

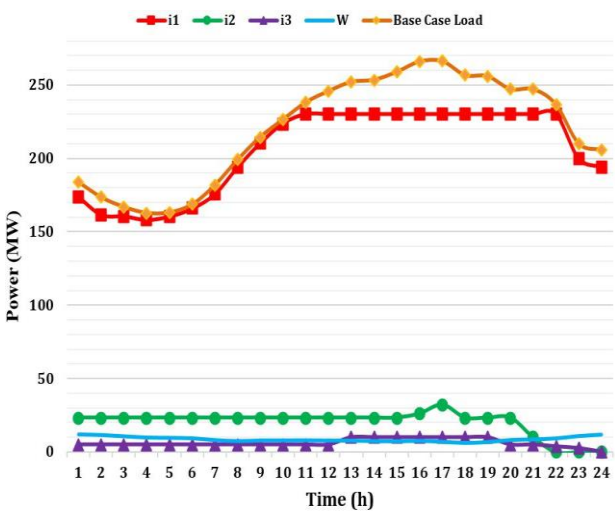


Fig. 8. Generation dispatch in Case 3.

3) Case 3

In this case, in addition to the presence of 10,000 EVs in the grid, their traveling patterns are taken into account according to Table VIII. In this case, in comparison to Case 2, at each bus, our developed EVs' model affects the balance between generation and consumption. The DC power flow is utilized in this case to examine the effects of the EVs' movable loads on the occurrence of the lines congestion and energy/reserve scheduling. In this case, EVs, as mobile loads, lead to rescheduling of generation through the whole grid due to line flow limits. In this condition, due to the traveling pattern of EVs, all of the busses of the system are seen as load busses. Therefore, in comparison to Case 2, the presence of EVs as mobile loads could affect the power flow so that Lines 4, 5, and 6 reach their maximum capacity. Consequently, in addition to more energy production, the congestion of these lines from adding the EVs lead to the increase of deploying more expensive reserves (from Generators 2 and 3), and also more involuntary load shedding. Consequently, in this case, the operation cost is 108354.06 $, which is increased by 6.15% and 3.79% in comparison to cases 1 and 2, respectively. The production schedule of thermal units is shown in Fig. 8.

4) Case 4

In this case, DRPs are considered in the day-ahead scheduling. Due to fast-response demand-side reserves, in the SCUC, a large portion of the generation-side reserve is replaced by DRPs. Consequently, the involuntary load shedding and the generation-side reserve decrease are reduced by about 64.64 and 28.48 percent, respectively, compared to Case 3. In this case, the operation cost is 105931.79 $, which shows 2.23% cost savings in comparison to Case 3.

5) Case 5

In this case, in the presence of the DR programs, the charge of the EVs is controlled by the system operator. According to Fig. 9, the peak hours occur between the intervals 13 to 21 wherein the reserve of the system is reduced to its minimum. Moreover, during this time period, almost all return trips of EVs have been completed and owners of vehicles tend to charge their cars immediately after the end of their journey. Therefore, with the massive entry of EVs' charging demand into the power system during this period, the security of the power system may be at risk.

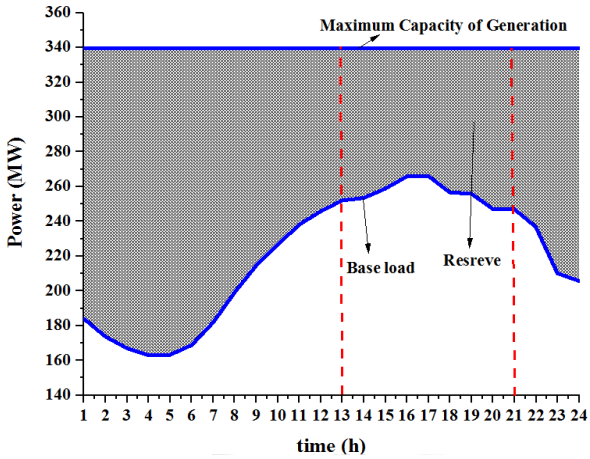


Fig. 9. Demand, reserve, and available generation capacity without EVs.

Here, to improve system reserve margin, two approaches are investigated and compared including controlled charging of EVs and utilizing the SL program. In the first one, the charging of EVs is shifted to non-peak periods and is avoided during the time interval 13 to 21. In this case, the operation cost is 104258.27 $ that compared with case 3 decreases by 3.78%. On the other hand, when the SL program is utilized, the operation cost becomes 103413.11 $ that shows 4.56% cost saving compared to Case 3. By employing both approaches, operation cost becomes 101345.24 $ in which, cost reduction is considerable. The generation dispatch of the thermal units is similar to Case 1. The only difference is that the generation of Unit 1 at hours 3 to 6 increases by 75 MW. Also, the deployed reserves of generation side decrease and DRR increases. Comparing with Cases 1 and 2, the deployed reserves of generation side decrease by 60% and 79.23% respectively. Table IX presents the scheduled SL program and Table X illustrates the operation cost of the system in detail. Also, Fig. 10 and Fig. 11 show the scheduled reserves in all cases and the scheduled $EU_{e,t}$ respectively.

TABLE IX
THE SCHEDULED SL LOAD IN CASE 5 (MW)

Shiftable Load	Bus 3	Bus 4	Bus 5
$SL_j^{17,4}$	2.50	6.20	10.39
$SL_j^{16,5}$	2.06	5.23	10.00
$SL_j^{15,3}$	2.16	6.91	9.43
$SL_j^{18,4}$	2.02	6.72	10.84
$SL_j^{19,6}$	2.20	6.67	10.01

TABLE X
SIX-BUS SYSTEM COSTS ($)

Case	Start-up and generation	Spinning and regulation	DR programs	Involuntary load shedding	Total cost
Case 1	99061	2850	-	163.62	102074.62
Case 2	100595.82	3020.86	-	777.64	104394.32
Case 3	103239.44	4024.60	-	1090.02	108354.06
Case 4	102969.16	1900.23	676.79	385.61	105931.79
Case 5	100475.00	582.41	287.83	0.00	101345.24

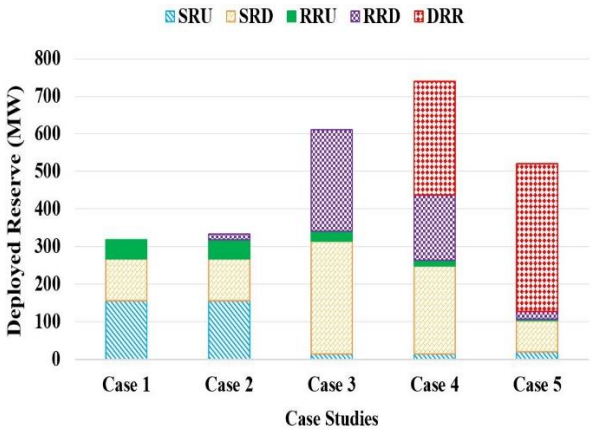


Fig. 10. Deployed reserves in case studies.

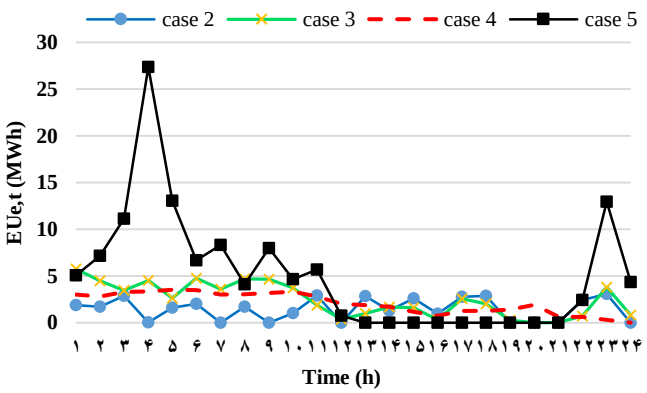


Fig. 11. The scheduled $EU_{e,t}$ in four cases.

E. Impact of different EV penetration levels on the operation cost and grid load

To investigate the impact of the EV penetration level on the proposed model, it is run for the different numbers of EVs in the power system for Case 5. Table XI shows different EV penetration levels regarding the different numbers of EVs in the power system.

Fig. 12 depicts the impact of different EV penetration levels on the operation cost. According to Table XI, as EVs penetration is growing, the number of EVs in the system is increasing. Consequently, because EVs have been modeled as mobile load, the operation cost of the system increases when different numbers of EVs penetration are added to the system.

TABLE XI
EV PENETRATION LEVELS (IN PERCENT) AND THE CORRESPONDING NUMBER OF EVS

EV Penetrates	Number of EVs
0 %	0
20 %	30200
40 %	60400
60 %	90600
80 %	120800
100 %	151000

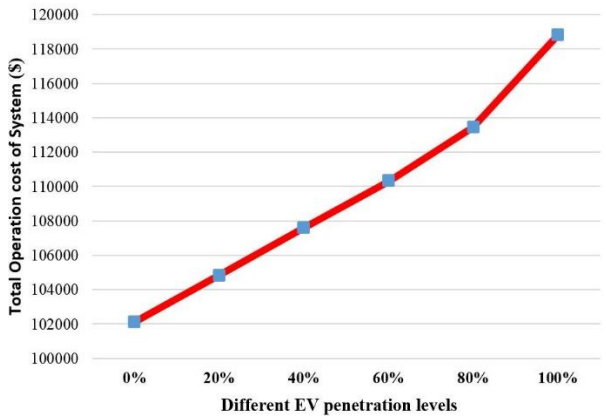


Fig. 12. Impact of different EV penetration levels on operation cost of power system.

Fig. 13 demonstrates the impact of different EV penetration levels on the total load of the system. According to Fig. 13, when the number of EVs in the grid increases, the load of the system is grown, which causes that more expensive units will be committed to provide more energy and reserve. This results the increment of the operating costs.

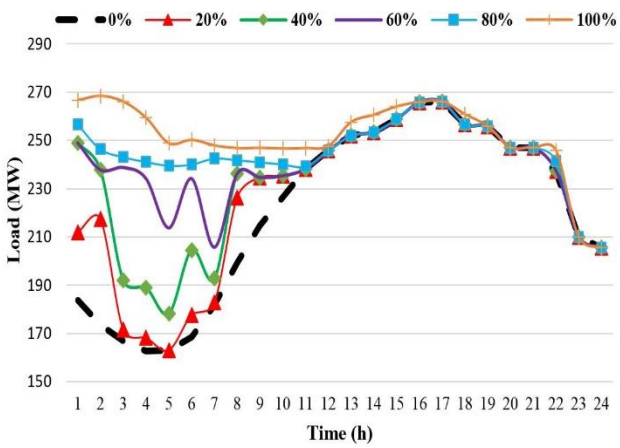


Fig. 13. Effect of different EV penetration levels on the load of system.

IV. CONCLUSIONS

In this paper, the SCUC problem was formulated as a stochastic MILP model that considers the effect of EVs' charging demand and the uncertainties of wind power and load. Using this model, the impacts of the presence of EVs, as mobile loads, on the system load and operation cost were investigated for different case studies. Moreover, it was shown that employing DR programs can facilitate the integration of the EVs into the power system by reducing load shedding, providing operating reserve, releasing line congestion and preventing scheduling expensive units for providing energy and reserve. Sensitivity analysis indicates that by increasing EV penetration into the power system, the system operation cost will be increased due to the commitment of more expensive generating units. However, this can be managed by the participation of various DR programs. As a part of future work, the authors are interested in modeling the impact of V2G technology on the presented SCUC problem.

ACKNOWLEDGMENT

The authors acknowledge the funding support of Babol Noshirvani University of Technology through Grant program No. BNUT/370162/98.

REFERENCES

[1] R. Lotfi, A. Mostafaeipour, N. Mardani, and S. Mardani, "Investigation of wind farm location planning by considering budget constraints," *Int. J. Sustain. Energy*, vol. 37, no. 8, pp. 799–817, Feb. 2018.

[2] M. Duvall et al., "Transportation Electrification: A Technology Overview," *Electric Power Research Institute* June. 2011.

[3] A. I. Negash, T. W. Haring, and D. S. Kirschen, "Allocating the cost of demand response compensation in wholesale energy markets," *IEEE Trans. Power Syst*., vol. 30, no. 3, pp. 1528–1535, May. 2015.

[4] J. Aghaei, and M. I. Alizadeh, "Demand Response in Smart Electricity Grids Equipped with Renewable Energy Sources: A Review," Renew. Sustain. Energy Reviews, vol. 18, pp. 64-72, Feb. 2013.

[5] M. Alhaider, L. Fan, and Z. Miao, "Benders Decomposition for stochastic programming-based PV/Battery/HVAC planning," IEEE Power Energy Soc. Gen. Meet., vol. 2016-Novem, 2016.

[6] M. Honarmand, A. Zakariazadeh and S. Jadid, "Integrated scheduling of renewable generation and electric vehicles parking lot in a smart microgrid," Energy Conversion and Management, vol. 86, pp. 745-755, Oct. 2014.

[7] C. Shaoand, X. Wang, X. Wang, C. Du, C. Dang and S. Liu "Cooperative Dispatch of Wind Generation and Electric Vehicles With Battery Storage Capacity Constraints in SCUC," IEEE Transaction on Smart Grid, vol. 5, no. 5, pp. 2219-2226, Sep. 2014.

[8] Q. Cai, Z. Xu, F. Wen, L. L. Lai and K. P. Wong. "Security Constrained Unit Commitment-based Power System Dispatching with Plug-in Hybrid Electric Vehicles," IEEE 13th International Conference on Industrial Informatics (INDIN), pp. 1014-1021, Jul. 2015.

[9] C. Shao, X. Wang, M. Shahidehpour, X. Wang, B. Wang. "Security-Constrained Unit Commitment with Flexible Uncertainty Set for Variable Wind Power," IEEE Transactions on Sustainable Energy, vol. 8, no. 3, pp. 1-9, Feb. 2017.

[10] J. Zhao, C. Wan, Z. Xu, K. P. Wong. "Spinning Reserve Requirement Optimization Considering Integration of Plug-

in Electric Vehicles," IEEE Transaction on Smart Grid, vol. 8, no. 4, pp. 2009-2021, June. 2016.
[11] H. Wu, M. Shahidehpour, A. Alabdulwahab and A. Abusorrah. "Demand Response Exchange in the Stochastic Day-Ahead Scheduling With Variable Renewable Generation," IEEE Transactions on Sustainable Energy, vol. 6, no. 2, pp. 1-10, Apr. 2015.
[12] C. Liu, J. Wang, A. Botterud, Y. Zhou and A. Vyas. "Assessment of Impacts of PHEV Charging Patternson Wind-Thermal Scheduling by Stochastic Unit Commitment," IEEE Transaction on Smart Grid, vol. 3, no. 2, pp. 675-683, Jun. 2012.
[13] M. E. Khodayar, L. Wu and M. Shahidehpour. "Hourly Coordination of Electric Vehicle Operation and Volatile Wind Power Generation in SCUC," IEEE Transactions on Smart Grid, vol. 3, no. 3, pp. 1271-1279, Sep. 2012.
[14] N. Neyestani, M. Y. Damavandi and G. Chicoo, "Effects of PEV Traffic Flows on the Operation of Parking Lots and Charging Stations," IEEE Transactions on Smart Grid, vol. 9, no. 2 , pp. 1521-1530, July. 2017.
[15] D. Madzharov, E. Delarue, W. Dhaeseleer, "Integrating electric vehicles as flexible load in unit commitment modeling," Energy, vol. 65, pp. 285-294, June. 2013.
[16] C. Sahin, M. Shahidehpour and I. Erkmen, "Allocation of Hourly Reserve versus Demand Response for Security-Constrained Scheduling of Stochastic Wind Energy," IEEE Transactions on Sustainable Energy, vol. 4, pp. 219-228, Jan. 2013.
[17] M. Ramezanzade, M. Jafari-Nokandi, T. Barforoshi, "Scheduling of generation and reserve of thermal generation resources considering load and wind uncertainty in presence of energy storage and demand response," TABRIZ Journal of Electrical Engineering, vol. 48, vol. 2, no. 84, pp. 653-665, 2018.
[18] G. Morales-España, Á. Lorca, and M. M. de Weerdt, "Robust unit commitment with dispatchable wind power," Electr. Power Syst. Res., vol. 155, no. February, pp. 58–66, Feb. 2018.
[19] Z. Yang, K. Li, Q. Niu, and Y. Xue, "A comprehensive study of economic unit commitment of power systems integrating various renewable generations and plug-in electric vehicles," Energy Convers. Manag., vol. 132, pp. 460–481, Jun. 2017.
[20] M. Shahbazitabar and H. Abdi, "A novel priority-based stochastic unit commitment considering renewable energy sources and parking lot cooperation," Energy, vol. 161, pp. 308–324, Oct. 2018.
[21] M. A. Mirzaei, A. S. Yazdankhah, and B. Mohammadi-Ivatloo, "Integration of Demand Response and Hydrogen Storage System in Security Constrained Unit Commitment with High Penetration of Wind Energy," 26th Iran. Conf. Electr. Eng. ICEE 2018, pp. 1203–1208, 2018.
[22] M. Hosseini Imani, M. Jabbari Ghadi, S. Shamshirband, and M. Balas, "Impact Evaluation of Electric Vehicle Parking on Solving Security-Constrained Unit Commitment Problem," Math. Comput. Appl., vol. 23, no. 1, p. 13, March. 2018.
[23] M. A. Mirzaei, A. Sadeghi Yazdankhah, and B. Mohammadi-Ivatloo, "Stochastic security-constrained operation of wind and hydrogen energy storage systems integrated with price-based demand response," Int. J. Hydrogen Energy, vol. 44, no. 27, pp. 14217–14227, May. 2019.
[24] M. H. Imani, K. Yousefpour, M. J. Ghadi, and M. T. Andani, "Simultaneous presence of wind farm and V2G in security constrained unit commitment problem considering uncertainty of wind generation," 2018 IEEE Texas Power Energy Conf. TPEC 2018, vol. 2018–Febru, pp. 1–6, Feb. 2018.
[25] Y. Sun, J. Dong, and L. Ding, "Optimal day-ahead wind-thermal unit commitment considering statistical and predicted features of wind speeds," Energy Convers. Manag., vol. 142, pp. 347–356, Jun. 2017.
[26] K. H. Jo and M. K. Kim, "Stochastic unit commitment based on multi-scenario tree method considering uncertainty," Energies, vol. 11, no. 4, March. 2018.
[27] https://www.iea.org/reports/global-ev-outlook-2019
[28] K. W. Hedman, M. C. Ferris, R. P. O'Neill, E. B. Fisher and S. S. Oren, "Co-optimization of Generation Unit Commitment and Transmission Switching with N-1 Reliability," IEEE Transactions on Power Systems, vol. 25, pp. 1052-1063, June. 2010.
[29] M. A. Ortega-Vazquez and D. S. Kirschen, "Estimating the Spinning Reserve Requirements in Systems with Significant Wind Power Generation Penetration," IEEE Transaction on Power Systems, vol. 22, no. 1, pp. 24-33, March. 2009.
[30] A. J. Conejo, M. Carrión and J. M. Morales, Decision Making under Uncertainty in Electricity Markets, Springer, New York, 2010.
[31] S. M. Hossein. Imani, S. Asghari, and M. T. Ameli. "Considering the Load Uncertainty for Solving Security Constrained Unit Commitment Problem in Presence of Plug-in Electric Vehicle," *The 22nd Iranian Conference on Electrical Engineering (ICEE)*, pp. 725-732, May 2014.



Mohsen Ramezanzade was born in Bojnord, Iran. He received his B.S. degree in Power Engineering from Noushirvani University of Technology , Babol, Iran in 2014, and his M.S. degree in Power System Engineering from Noushirvani University of Technology , Babol, Iran in 2016. His research interests are power system operation and economics, power system planning, and Renewable Energy Resources and environment issue.



Meysam Jaefari-Nokandi received the B.Sc degree from Sharif University of Technology, Tehran, Iran, in 2003 and the M.Sc and Ph.D degree from University of Tehran, Tehran, Iran, in 2005 and 2011, respectively, both in electrical engineering. He has joined faculty of Electrical and Computer Engineering, Babol Noshirvani University of Technology since 2011.His research interests are power market and power system reliability, operation and planning.



Taghi Barforoushi received the B.Sc. degree in electrical engineering from Iran University of Science and Technology, Tehran, Iran, in 1994 and the M.Sc. and Ph.D. degrees from Tarbiat Modares University, Tehran, in 1999 and 2008, respectively. He worked at Mazandaran Regional Electric Company (MREC) from April 1999 to May 2012. He is currently an assistant professor with the faculty of electrical and computer engineering, Babol Noshirvani University of Technology, Babol, Iran. His research interests are power system planning and operation, Electricity markets.



Javad Saebi received the B.Sc. degree in electrical engineering from Iran University of Science and Technology, Tehran, Iran, in 2007, the M.Sc. degree from University of Tehran, Tehran, Iran, in 2009, and the Ph.D. degree from Ferdowsi University of Mashhad, Mashhad, Iran, in 2015. He is currently an assistant professor with the faculty of electrical engineering, University of Bojnord, Bojnord, Iran. His research interests include smart grid, renewable energy, power system planning and operation and power markets.